Polymers in turbulence: stretching statistics and the role of extreme strain-rate fluctuations

Jason R Picardo, Emmanuel L.C. Vi M. Plan, Dario Vincenzi

Polymers in turbulence: stretching statistics and the role of extreme strain-rate fluctuations

Jason R. Picardo[1]†, Emmanuel L. C. VI M. Plan[2] and Dario Vincenzi[3]‡

[1]Department of Chemical Engineering, Indian Institute of Technology Bombay, Mumbai, 400076, India

[2]Hanoi School of Business and Management, Vietnam National University, Ha Noi, 100 000, Vietnam

[3]Université Côte d'Azur, CNRS, LJAD, 06000 Nice, France

Polymers in a turbulent flow are stretched out by the fluctuating velocity gradient and exhibit a broad distribution of extensions R; the *stationary* probability distribution function (p.d.f.) of R has a power-law tail with an exponent that increases with the Weissenberg number Wi, a nondimensional measure of polymer elasticity. This study addresses the following questions: (i) What is the role of the non-Gaussian statistics of the turbulent velocity gradient on polymer stretching? (ii) How does the p.d.f. of R evolve to its asymptotic stationary form? Our analysis is based on simulations of the dynamics of finitely-extensible bead-spring dumbbells and chains, in the extremely dilute limit, that are transported in a homogeneous and isotropic turbulent flow, as well as in a Gaussian random flow. First, we recall the large deviations theory of polymer stretching, and illustrate its application. Then, we show that while the turbulent flow is more effective at stretching small-Wi stiff polymers, the Gaussian flow is more effective for high-Wi polymers. This suggests that high-Wi polymers (with large relaxation times) are primarily stretched by the cumulative effect of moderate strain-rate events, rather than by short-lived extreme-valued strain rates; we confirm this behaviour by analysing the persistence time of polymers in stretched states. Next, we show that, beginning from a distribution of coiled polymers, the p.d.f. of R exhibits two distinct regimes of evolution. At low to moderate Wi, the p.d.f. quickly develops a power-law tail with an exponent that evolves in time and approaches its stationary value exponentially. This result is supported by an asymptotic analysis of a stochastic model. At high Wi, the rapid stretching of polymers first produces a peak in the p.d.f. near their maximum extension; a power law with a constant exponent then emerges and expands its range towards smaller R. The time scales of equilibration, measured as a function of Wi, point to a critical slowing down at the coil-stretch transition. Importantly, these results show no qualitative change when chains in a turbulent flow are replaced by dumbbells in a Gaussian flow, thereby supporting the use of the latter for reduced-order modelling.

Key words: Polymers; Isotropic turbulence

1. Introduction

The non-Newtonian behaviour of turbulent polymer solutions results from the stretching of polymer molecules dissolved in the fluid. A detailed understanding of the statistics of polymer stretching in turbulent flows is, therefore, essential to explain phenomena such as turbulent drag reduction (Graham 2014; Benzi & Ching 2018; Xi 2019) and elastic turbulence (Steinberg

† Email address for correspondence: jrpicardo@che.iitb.ac.in; Also, Associate, International Centre for Theoretical Sciences, TIFR, India.

‡ Also, Associate, International Centre for Theoretical Sciences, TIFR, India.

2021). On the flip side, extreme stretching causes the mechanical scission of polymers, following which all non-Newtonian effects are lost (Soares 2020). To accurately model scission and the consequent loss of viscoelasticity, we must understand how the turbulent flow stretches out individual polymers to large extensions.

The strain rate in a turbulent flow fluctuates in magnitude and orientation. In addition, vorticity constantly rotates the polymers and prevents them from persistently aligning with the stretching eigendirection of the strain-rate tensor. Nonetheless, Lumley (1973) predicted that a turbulent flow can stretch polymers, if the product of the mean-square strain rate and its Lagrangian integral time exceeds the inverse of the elastic relaxation time of the polymers. The Lagrangian numerical simulations of Massah *et al.* (1993) confirmed the unravelling of individual bead-spring chains in a turbulent channel flow, while Groisman & Steinberg (2001) provided experimental evidence of this phenomenon in elastic turbulence: The transition from a laminar shear flow to a chaotic flow was found to coincide with a dramatic increase in the polymer-induced shear stress.

A systematic theory of polymer stretching in turbulent flows was developed by Balkovsky, Fouxon & Lebedev (2000, 2001) and Chertkov (2000) using the methods of dynamical systems. One of the main results is that the end-to-end extension R of the polymer has a stationary probability density function (p.d.f.), $p(R)$, that behaves as a power law $R^{-1-\alpha}$ for R between the equilibrium and contour lengths of the polymer. The exponent α is a function of the Weissenberg number Wi, defined as the product of the Lyapunov exponent of the flow and the polymer relaxation time; this relationship is expressed in terms of the Cramér function that describes the large deviations of the stretching rate of the flow. Note that the power-law behaviour of $p(R)$ is a distinctive feature of turbulent flows—the distribution of polymer extensions remains broad even at large strain rates—and is not observed in laminar, extensional flows (Perkins, Smith & Chu 1997; Nguyen & Kausch 1999; Schroeder 2018).

The power-law behavior of the p.d.f. of R has been confirmed in various flow configurations: experimentally by direct observation of individual polymers in elastic turbulence (Gerashchenko, Chevallard & Steinberg 2005; Liu & Steinberg 2010, 2014); and numerically in shear turbulence (Eckhardt, Kronjäger & Schumacher 2002; Puliafito & Turitsyn 2005), in two- and three-dimensional isotropic turbulence (Boffetta, Celani & Musacchio 2003; Watanabe & Gotoh 2010; Gupta, Perlekar & Pandit 2015; Rosti, Perlekar & Mitra 2021), and in turbulent channel and pipe flows (Bagheri *et al.* 2012; Serafini *et al.* 2022). This study further investigates the power-law behaviour of $p(R)$ by examining (i) how polymer stretching is affected by the extreme velocity gradient fluctuations that characterize turbulence and (ii) how the p.d.f. of R evolves from an initial distribution of coiled polymers to its stationary profile.

Typically, the contour length of the polymer is smaller than the viscous scale of the turbulent flow, and so polymer deformation is entirely determined by the statistics of the velocity gradient (Ilg *et al.* 2002; Stone & Graham 2003; Zhou & Akhavan 2003; Gupta, Sureshkumar & Khomami 2004; Terrapon *et al.* 2004; Peters & Schumacher 2007). It is natural, therefore, to consider simplifying the simulation of polymer stretching by using a random velocity gradient model with appropriate statistics. This would facilitate the testing and development of advanced polymer models, beyond the simple dumbbell or freely-jointed chain, by avoiding expensive direct numerical simulations (DNS) of the carrier flow. However, one must first answer the question: Does stochastic modelling of the turbulent flow modify, in a fundamental way, the stretching dynamics of polymers?

In the broader context of the turbulent transport of anisotropic particles, several studies have shown that particle-orientation dynamics cannot be explained fully by using Gaussian models of the velocity gradient (see, *e.g.*, Pumir & Wilkinson 2011; Chevillard & Meneveau 2013; Gustavsson, Einarsson & Mehlig 2014; Anand, Ray & Subramanian 2020). Meanwhile, for single-polymer dynamics, Gaussian velocity-gradient models have undoubtedly been useful in gaining a qualitative understanding of stretching statistics (*e.g.* Shaqfeh & Koch 1992; Mosler & Shaqfeh

1997; Chertkov 2000; Martins Afonso & Vincenzi 2005; Puliafito & Turitsyn 2005; Vincenzi *et al.* 2021). To our knowledge, however, the effect of the strongly non-Gaussian fluctuations of a turbulent velocity gradient on the statistics of R, and in particular on the dependence of α upon Wi, has not yet been investigated. With this aim, we carry out Lagrangian numerical simulations of finitely extensible nonlinear elastic (FENE) dumbbells in three-dimensional isotropic turbulence, as well as in a Gaussian model of the velocity gradient, and compare the statistics of R. This investigation has relevance beyond stochastic modelling, because flows without extreme strain-rates arise naturally in the context of polymer solutions—wherein polymer-feedback forces suppress extreme velocity-gradient fluctuations (Perlekar, Mitra & Pandit 2010; Watanabe & Gotoh 2013; ur Rehman, Lee & Lee 2022).

So far, most studies have focused on the stationary statistics of polymer extensions. However, the transient dynamics is important in situations where polymer scission occurs and the long-time stationary state may never be reached (Soares 2020). In addition, the finite-time statistics of polymer stretching is relevant to experimental measurements, which are necessarily limited in their duration, as well as to the calibration of numerical simulations. The characteristic time required for polymers to equilibrate in a turbulent flow has been studied in stochastic models (Martins Afonso & Vincenzi 2005; Celani, Puliafito & Vincenzi 2006) and isotropic turbulence (Watanabe & Gotoh 2010). A significant slowing down of the stretching dynamics has been found near the coil–stretch transition. This phenomenon is reminiscent of the slowing down observed in an extensional flow (Gerashchenko & Steinberg 2008), but has a different origin. Specifically, it is not a consequence of the conformation hysteresis typical of extensional flows (Schroeder *et al.* 2003, 2004), but rather arises from the strong heterogeneity of polymer configurations in the vicinity of the coil–stretch transition (Celani *et al.* 2006). Other than the equilibration time, little is known about how the p.d.f. of polymer extension approaches its asymptotic shape and, in particular, whether or not the power-law behaviour appears at earlier times. Here, this issue is studied by means of Lagrangian simulations of single-polymer dynamics in three-dimensional isotropic turbulence; simulations for both a dumbbell and a bead-spring chain are compared. In addition, the numerical results are explained by using a Fokker–Planck equation for the time-dependent p.d.f. of R.

The dumbbell model of polymers is presented in § 2, along with a description of the Lagrangian simulations that form the basis of this study. The random and turbulent carrier flows are also described there. Section 3 focuses on the stationary p.d.f. of polymer extensions. In § 3.1, the theory of Balkovsky *et al.* (2000) and Chertkov (2000) is recalled briefly and is illustrated by using a renewing Couette flow. Section 3.2 then examines the effect of the non-Gaussian statistics of a turbulent velocity gradient on polymer stretching. Section 4 is devoted to understanding the temporal evolution of the p.d.f. of polymer extensions, with the aid of a stochastic model. We then verify, in § 5, that the results obtained for the elastic dumbbell remain true even for chains with a larger number of beads. Finally, we conclude in § 6 with a summary of our study and a discussion of its implications.

2. Lagrangian simulations in random and turbulent flows

2.1. *Dumbbell model*

We primarily model polymer molecules using the finitely extensible nonlinear elastic (FENE) dumbbell model (Bird *et al.* 1987; Öttinger 1996; Graham 2018). With τ as the relaxation time of the polymer, R_{eq} as the equilibrium root-mean-square (r.m.s.) end-to-end length, and R_m as the

maximum length, the dynamics of the end-to-end separation vector $\boldsymbol{R}$ in d dimensions satisfies

$$\frac{\mathrm{d}\boldsymbol{R}}{\mathrm{d}t} = \boldsymbol{\kappa}(t) \cdot \boldsymbol{R} - f(R)\frac{\boldsymbol{R}}{2\tau} + \sqrt{\frac{R_{\mathrm{eq}}^2}{\tau d}}\,\boldsymbol{\xi}(t), \qquad (2.1)$$

where $\kappa_{ij} = \nabla_j u_i$ is the velocity gradient at the location of the centre of mass of the polymer, $f(R) = \left(1 - R^2/R_m^2\right)^{-1}$ defines the FENE spring force, and $\boldsymbol{\xi}(t)$ is d-dimensional white noise that accounts for thermal fluctuations. This noise would also make an appearance in the equation of motion for the centre of mass. However, its effect on the transport of the dumbbell is very small compared to the advection by the turbulent carrier flow and thus may be neglected. The motion of the centre of mass of the polymer is therefore treated like that of a tracer.

Given a Lagrangian time series of $\boldsymbol{\kappa}(t)$, (2.1) is integrated using the Euler–Marujama method supplemented with the rejection algorithm proposed by Öttinger (1996), which rejects those time steps that yield extensions greater than $R_m\left(1 - \sqrt{\mathrm{d}t/10}\right)^{1/2}$. Since the velocity gradient fluctuates, the numerical integration of (2.1) does not present the same difficulties as in the case of a laminar extension flow, and more sophisticated integration methods are not necessary. We have indeed checked that only a negligible fraction of time steps is rejected over a simulation.

Throughout this paper, we study the dumbbell model with $R_{\mathrm{eq}} = 1$ and $R_m = 110$. The elastic relaxation time τ defines the non-dimensional Weissenberg number, $Wi \equiv \lambda\tau$, where λ is the maximum Lyapunov exponent of the carrier flow. The Weissenberg number provides a non-dimensional measure of the elasticity of the polymer, with high-Wi polymers being easily extensible. We consider a wide range of Wi, from 0.3 to 40.

Note that while the dumbbell model (2.1) is used in most of this study, we do show in § 5 that our results also hold true for bead-spring chains.

2.2. *Turbulent carrier flow*

To study polymer stretching in a turbulent flow, we use a database of Lagrangian trajectories from a DNS of homogeneous isotropic incompressible turbulence (at Taylor-microscale Reynolds number $Re_\lambda \approx 111$), generated at ICTS, Bangalore (James & Ray 2017). The DNS solves the incompressible Navier–Stokes equations, discretized on a periodic cube, using a standard fully-dealiased pseudo-spectral method with 512^3 grid points. Time integration is performed using a second-order slaved Adams–Bashforth scheme. The motion of 9×10^5 tracers is calculated using a second-order Runge–Kutta method for time integration; the fluid velocity at the location of a tracer is obtained from its value on the grid using trilinear interpolation. The velocity gradient $\boldsymbol{\nabla u}$ is calculated along these trajectories and stored at intervals of $0.11\tau_\eta$, where τ_η is the Kolmogorov time-scale (given below). This Lagrangian data provides the values of $\boldsymbol{\kappa}(t)$ for the integration of (2.1) along 9×10^5 trajectories, allowing us to obtain good statistics of single-polymer stretching dynamics.

The Lyapunov exponent of the flow, required for defining Wi, is computed from these trajectories via the continuous QR method, implemented using an Adams–Bashforth projected integrator along with the composite trapezoidal rule (for further details see Dieci *et al.* 1997). We find $\lambda = 0.136/\tau_\eta$ which is compatible with previous simulations of isotropic turbulence (Bec *et al.* 2006). We also estimate the Lagrangian correlation time-scales of strain-rate and vorticity in the turbulent flow, τ_S and τ_Ω, which serve as inputs to the Gaussian random model described in the next subsection. The rate-of-strain and rotation tensors are defined as $\boldsymbol{S} = (\boldsymbol{\nabla u} + \boldsymbol{\nabla u}^\top)/2$ and $\Omega = (\boldsymbol{\nabla u} - \boldsymbol{\nabla u}^\top)/2$, respectively. The autocorrelation functions of S_{11} and Ω_{12} are calculated and found to display an approximately exponential decay. Integrating these functions yields the integral time scales $\tau_S = 2.20\,\tau_\eta$ and $\tau_\Omega = 8.89\,\tau_\eta$, in agreement with previous numerical simulations at comparable R_λ (Yeung 2001). The Kolmogorov time-scale τ_η is determined from S_{11}, using isotropy, as $\tau_\eta = \left(15\langle S_{11}^2\rangle\right)^{-1/2} = 3.72 \times 10^{-2}$.

<div align="center">2.3. Gaussian random velocity gradient</div>

One of the goals of this study is to compare the stretching of polymers in a turbulent flow to that in a flow with Gaussian statistics, in order to determine the effect of extreme-valued fluctuations of the turbulent velocity gradient. For this, we use a Gaussian random velocity-gradient model to generate a time series of $\kappa(t)$ for each polymer trajectory. Following Brunk, Koch & Lion (1997), we take $\kappa(t) = \boldsymbol{S}(t) + \Omega(t)$ with

$$
\boldsymbol{S} = \sqrt{3}\,A \begin{pmatrix} \frac{2\zeta_1}{\sqrt{3}} & \zeta_3 & \zeta_4 \\ \zeta_3 & -\frac{\zeta_1}{\sqrt{3}} + \zeta_2 & \zeta_5 \\ \zeta_4 & \zeta_5 & -\frac{\zeta_1}{\sqrt{3}} - \zeta_2 \end{pmatrix}, \qquad \Omega = \sqrt{5}\,A \begin{pmatrix} 0 & \varpi_1 & \varpi_2 \\ -\varpi_1 & 0 & \varpi_3 \\ -\varpi_2 & -\varpi_3 & 0 \end{pmatrix}, \qquad (2.2)
$$

where A determines the magnitude of the velocity gradient and $\zeta_i(t)$ $(i = 1, \ldots, 5)$ and $\varpi_i(t)$ $(i = 1, 2, 3)$ are independent zero-mean unit-variance Gaussian random variables with exponentially decaying autocorrelation functions and integral times τ_S and τ_Ω, respectively. Therefore, S_{ij} and Ω_{ij} are Gaussian variables such that $\langle S_{ij} \rangle = \langle \Omega_{ij} \rangle = 0$,

$$
\langle S_{ik}(t) S_{jl}(0) \rangle = 3A^2 \left(\delta_{ij}\delta_{kl} + \delta_{il}\delta_{jk} - \frac{2}{3}\delta_{ik}\delta_{jl} \right) e^{-t/\tau_S}, \qquad (2.3)
$$

and

$$
\langle \Omega_{ik}(t) \Omega_{jl}(0) \rangle = 5A^2 \left(\delta_{ij}\delta_{kl} - \delta_{il}\delta_{jk} \right) e^{-t/\tau_\Omega}. \qquad (2.4)
$$

As a consequence, $\langle \Omega_{ij}\Omega_{ij} \rangle = \langle S_{ij}S_{ij} \rangle$, which reproduces the relation $\nu \langle \omega^2 \rangle = \langle \epsilon \rangle$, where ω is the vorticity and ϵ is the energy dissipation rate (Frisch 1995). We take τ_S and τ_Ω to be the same as in the turbulent flow (§ 2.2). Furthermore, we set the coefficient $A = 2.538$ so as to obtain approximately the same Lyapunov exponent λ as in the turbulent flow. As a consequence, the Kubo number $Ku = \lambda\tau_S$ is also nearly the same in the turbulent and Gaussian flows.

3. Stationary statistics of polymer stretching

We begin our study by considering the long-time, statistically stationary distribution of the end-to-end extension of polymers. We first recall the large deviations theory of Balkovsky *et al.* (2000) and Chertkov (2000), which not only predicts a power-law tail in the p.d.f of R, but also provides a way to calculate the corresponding exponent for any chaotic carrier flow, given sufficient knowledge of its dynamical properties. We illustrate the predictive capability of the theory for a simple, analytically specified, renewing flow. Unfortunately, direct application of the theory to turbulent flows is impractical and one must typically resort to approximations, such as considering the turbulent flow to be decorrelated in time. Such considerations will naturally lead us to examine how and to what extent the time-correlated, non-Gaussian nature of turbulent flow statistics impacts polymer stretching.

<div align="center">3.1. Large deviations theory: illustration for a renewing flow</div>

The theory of Balkovsky *et al.* (2000) and Chertkov (2000) is recalled here in terms of the generalized Lyapunov exponents, rather than the Cramér function of the strain rate; the two properties are equivalent and related via a Legendre transform (see Boffetta, Celani & Musacchio 2003). If $\boldsymbol{\ell}(t)$ is a line element in a random flow, the Lyapunov exponent is defined as

$$
\lambda = \lim_{t \to \infty} \frac{1}{t} \left\langle \ln \left[\frac{\ell(t)}{\ell(0)} \right] \right\rangle, \qquad (3.1)
$$

where $\langle \cdot \rangle$ denotes the average over the statistics of the velocity field. The q-th generalized Lyapunov exponent,

$$\mathscr{L}(q) = \lim_{t \to \infty} \frac{1}{t} \ln \left\langle \left[\frac{\ell(t)}{\ell(0)} \right]^q \right\rangle, \tag{3.2}$$

gives the asymptotic exponential growth rate of the q-th moment of $\ell(t)$. The function $\mathscr{L}(q)$ is positive and convex and satisfies $\mathscr{L}'(0) = \lambda$ (see, *e.g.*, Cecconi, Cencini & Vulpiani 2010, for more details). If the flow is incompressible, then we also have $\mathscr{L}(-d) = \mathscr{L}(0) = 0$, where d is the space dimension (Zel'dovich *et al.* 1984).

For the elastic dumbbell (2.1), the p.d.f of the extension has a power-law form, $p(R) \sim R^{-1-\alpha}$ for $R_{\mathrm{eq}} \ll R \ll R_m$, with an exponent that satisfies

$$\frac{\alpha}{2Wi} = \frac{\mathscr{L}(\alpha)}{\lambda}. \tag{3.3}$$

Given the properties of $\mathscr{L}(q)$, equation (3.3) implies that α is a decreasing function of Wi that crosses zero at the critical value $Wi_{\mathrm{cr}} = 1/2$ and saturates to $-d$ for very large Wi. In the limit $R_m \to \infty$, the p.d.f. of R ceases to be normalizable for $Wi \geqslant Wi_{\mathrm{cr}}$, *i.e.* highly stretched configurations predominate, and so Wi_{cr} is taken to mark the coil–stretch transition.

In principle (3.3) may be used to determine α as a function of Wi. However, in general, calculating the function $\mathscr{L}(q)$ is very challenging. A useful approximation can be obtained in the vicinity of the coil–stretch transition by expanding about $q = 0$: $\mathscr{L}(q) = \lambda q + \Delta q^2/2 + O(q^3)$ with $\Delta = \int \left(\langle \zeta(t)\zeta(t') \rangle - \lambda^2 \right) dt'$ and $\zeta(t) = \boldsymbol{R} \cdot \boldsymbol{\kappa}(t) \cdot \boldsymbol{R}/R^2$. Substituting this quadratic expansion into (3.3) yields

$$\alpha = \frac{\lambda}{\Delta} \left(\frac{1}{Wi} - 2 \right) \quad \text{for } Wi \to Wi_{\mathrm{cr}}. \tag{3.4}$$

Interestingly, in the limiting case of a time-decorrelated flow, (3.4) is accurate for all Wi, since $\mathscr{L}(q)$ is quadratic for all q (Falkovich, Gawędki & Vergassola 2001). Moreover, in this case $\lambda/\Delta = d/2$, which further simplifies (3.4) to yield:

$$\alpha = \frac{d}{2} \left(\frac{1}{Wi} - 2 \right). \tag{3.5}$$

To obtain α for polymers in a general chaotic flow and for arbitrary Wi, we must measure $\mathscr{L}(q)$; due to statistical errors this is especially difficult for values of q that are negative or large and positive (Vanneste 2010). Thus, past studies have been restricted to values of Wi sufficiently near Wi_{cr} so that α does not deviate far from zero (Gerashchenko *et al.* 2005; Bagheri *et al.* 2012). In order to illustrate the validity of (3.3) over a wider range of Wi, we now consider a renewing (or renovating) random flow, for which $\mathscr{L}(q)$ can be calculated easily (Childress & Gilbert 1995). To generate this flow, the time axis is divided into intervals $\mathscr{I}_n = [t_n, t_{n+1})$ with $t_n = n\tau_c$ and $n = 1, 2, \ldots$. The velocity field changes randomly at the beginning of each interval and then remains frozen for the rest of the time interval. Thus, the parameter τ_c sets the velocity correlation time. The velocity field is chosen to be a Couette flow, *i.e.* a two-dimensional linear shear flow, with a direction that is randomly rotated by an angle θ_n at the beginning of each time interval $\mathscr{I}_n$ (Young 1999, 2009). For $t \in \mathscr{I}_n$ the velocity gradient takes the form

$$\boldsymbol{\kappa} = \sigma \begin{pmatrix} -\sin\theta_n \cos\theta_n & \cos^2\theta_n \\ -\sin^2\theta_n & \sin\theta_n \cos\theta_n \end{pmatrix}, \tag{3.6}$$

where σ is the magnitude of the shear and θ_n is distributed uniformly over $[0, 2\pi]$. The Lyapunov exponent as well as the generalized Lyapunov exponents for this flow can be calculated
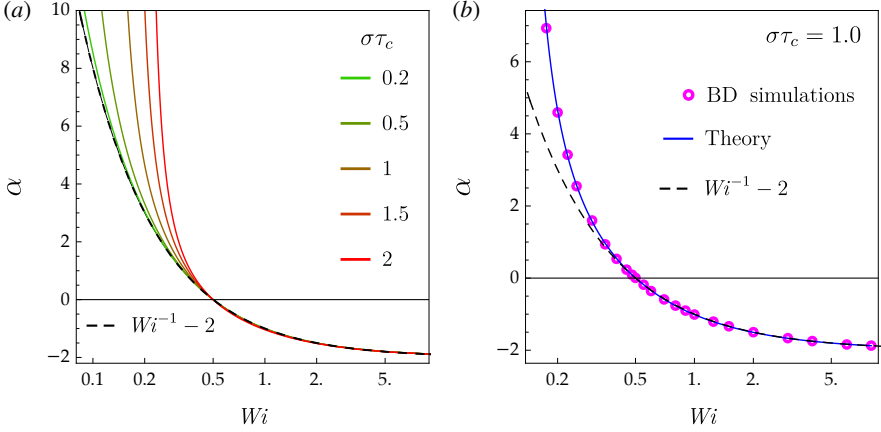
FIG. 1. (a) Slope of $p(R)$ as a function of Wi, as predicted by the large deviations theory, for the renewing Couette flow with various values of $\sigma\tau_c$. The dashed line is the prediction (3.5) for a time-decorrelated flow ($\tau_c = 0$) with $d = 2$. (b) Comparison of the large deviations theory (solid line) with BD simulations of the dumbbell model (markers), for the renewing Couette flow with $\sigma = 10$ and $\tau_c = 0.1$. The decorrelated flow (dashed line) is seen to provide a good approximation for Wi near to $Wi_{cr} = 1/2$ and beyond.

exactly (Young 1999, 2009):

$$\lambda = \frac{1}{2\tau_c}\ln\left(1 + \frac{\sigma^2\tau_c^2}{4}\right), \qquad \mathscr{L}(q) = \frac{1}{\tau_c}\ln\left[P_{q/2}\left(1 + \frac{\sigma^2\tau_c^2}{2}\right)\right], \tag{3.7}$$

where $P_{q/2}$ is the Legendre function of order $q/2$.

The solution of (3.3) for the renewing Couette flow is presented in figure 1(a) for several values of $\sigma\tau_c$ (this non-dimensional group is the only free parameter that remains after substituting (3.7) in (3.3)). As τ_c is decreased towards zero the results are seen to approach the prediction for a delta-correlated flow (3.5), shown by the dashed (black) line. We also expect the results for all cases of $\sigma\tau_c$ to be well approximated by (3.5) in the vicinity of the coil–stretch transition, $Wi = Wi_{cr} = 1/2$. This is indeed the case. In addition, for this renewing flow, (3.5) is seen to provide an excellent approximation for all Wi greater than Wi_{cr}. In general, one may expect the deviation of α from the prediction of (3.5) to be higher for small Wi than for large Wi. This is because α is negative for large Wi and the form of $\mathscr{L}(q)$ for negative arguments is strongly constrained by its convexity and the general properties $\mathscr{L}(0) = \mathscr{L}(-d) = 0$ and $\mathscr{L}'(0) = \lambda$.

In figure 1(b) the prediction of (3.3) is compared with the results of Brownian dynamics (BD) simulations of the dumbbell model (§ 2.1), with κ given by (3.6), for the case of $\tau_c = 0.1$ and $\sigma = 10$. The decorrelated-flow approximation is also shown for comparison (black dashed line). To obtain α from the simulations, we fit the stationary p.d.f of the extension $p(R)$ with a power law over a range $R_{eq} \ll R \ll R_m$. Figure 1(b) shows excellent agreement between the large deviations theory and the simulations of the dumbbell model.

It is interesting to note that (3.3) may also be regarded as a tool for measuring the generalized Lyapunov exponents of a turbulent flow from the statistics of polymer extensions. Since α is a monotonic function of Wi, one could invert the α vs Wi relation obtained from simulations and express Wi in terms of α on the left-hand-side of (3.3), so as to obtain an explicit formula for $\mathscr{L}(\alpha)$. However, even with this strategy, measuring the generalized Lyapunov exponents for large negative and positive orders will remain challenging. On the one hand, because $\alpha \geqslant -d$ this approach cannot yield the generalized Lyapunov exponents of order less than $-d$. On the other hand, it is computationally intensive to construct the tail of the p.d.f. of R for small Wi, which
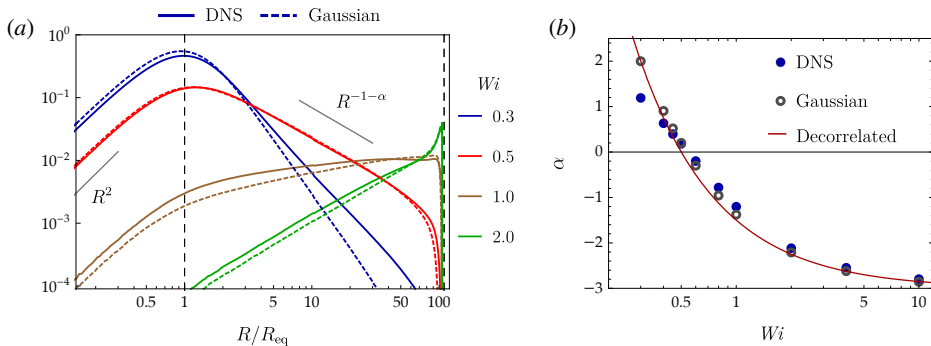
FIG. 2. Stationary probability distributions functions of the end-to-end extension R of polymers in turbulent and random flows. (a) Comparison of the stationary p.d.f. of R, for different values of Wi, in a DNS of turbulent flow and a synthetic Gaussian flow, constructed with the same Lyapunov exponent λ as the DNS, as well as the same Lagrangian correlation times for vorticity, τ_Ω, and strain rate, τ_S. (b) The power-law exponent of the tail of the p.d.f. of R (panel a) presented as a function of Wi. The exponents from DNS are compared with that from the Gaussian flow, as well as with the prediction for a three-dimensional time-decorrelated random flow in (3.5).

corresponds to large positive values of α and hence to generalized Lyapunov exponents of large positive order.

3.2. *Stretching in turbulence and the roles of mild and extreme strain rates*

Let us now examine the p.d.f. of the extension for FENE dumbbells in homogeneous isotropic turbulence (§ 2.2). These results are presented in figure 2(a) (solid lines). A power-law range is apparent for R between R_{eq} and R_m (vertical dashed lines) and the corresponding exponents, $-1-\alpha$, are seen to increase past -1 as Wi increases beyond Wi_{cr}. (The R^2 behaviour for $R < R_{eq}$ is a consequence of thermal fluctuations.) This panel also shows results for a Gaussian random flow (dotted lines), constructed so as to match the turbulent flow in terms of its integral correlation times of vorticity and strain as well as its Lyapunov exponent λ (see § 2.3). Of course, the higher-order generalized Lyapunov exponents of these two flows will not be the same (see Biferale, Meneveau & Verzicco 2014), and this is reflected in the differing values of α shown in figure 2(b) (markers). The thin solid line in this panel corresponds to the result (3.5) for a three-dimensional ($d = 3$) time-decorrelated random flow. Though small, the differences between these results show a systematic dependence on Wi which warrants further scrutiny.

Consider first the effect of the non-Gaussian statistics of turbulence. Figure 2(b) shows that low-Wi stiff polymers stretch more in a turbulent flow than in a Gaussian flow: the values of α are less negative in the turbulent flow (compare the filled and open markers) which implies a greater power-law exponent for $p(R)$. Therefore, encountering a higher frequency of extreme-valued velocity gradients aids in stretching stiff polymers. Surprisingly, this is no longer true when Wi is increased beyond Wi_{cr}. Rather, these moderately high-Wi polymers which are relatively easy to stretch are seen to be more extended in a Gaussian flow than in a turbulent flow. On further increasing Wi, all three flows in figure 2(b) eventually exhibit nearly identical values of α; this is to be expected since α must attain the limiting value of -3 regardless of flow statistics (see § 3.1).

Why are moderately high-Wi polymers stretched more in a Gaussian flow? To answer this, it is helpful to examine the p.d.f. of the rate of strain $s = \sqrt{S_{ij}S_{ij}}$ sampled by polymers. Figure 3(a) compares the distributions of s for the turbulent and Gaussian flows. We see that the Gaussian flow has a comparative abundance of mild strain-rate events to compensate for its lack of extreme-valued events. This suggests that high-Wi polymers that have long relaxation times are stretched more effectively by mild persistent straining rather than by strong but short-lived straining. In
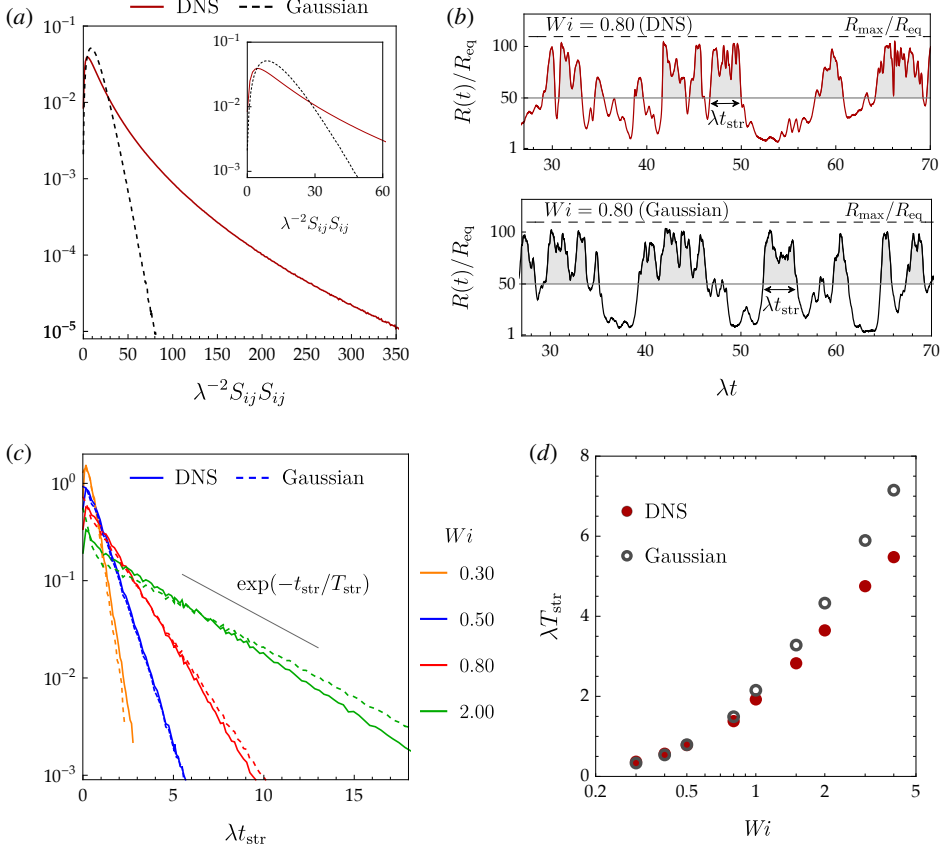
FIG. 3. Effect of non-Gaussian velocity-gradient fluctuations on polymer stretching in turbulence. (*a*) Comparison of the p.d.f. of the strain rate sampled by polymers in a DNS of turbulent flow with that in a synthetic Gaussian flow with same λ, τ_Ω, τ_S as the DNS. The inset is a zoom which shows the near-peak behaviour of the distributions. (*b*) Illustration of the typical stretching dynamics of a $Wi = 0.8$ polymer in the DNS (top panel) and Gaussian flow (bottom panel). The grey shading shows when the polymer is stretched beyond a threshold of $\ell = R_m/2 = 50$; each such time interval yields a value of t_{str}. (*c*) Distributions of t_{str} for various values of Wi in both DNS and Gaussian flows. The exponential tails of these p.d.f.s are associated with the time-scale T_{str}. (*d*) Variation of T_{str}, the typical time spent by polymers in a stretched state, as a function of Wi, for both DNS and Gaussian flows. High-Wi polymers in the Gaussian flow are seen to persist in a stretched state for significantly longer than they do in the DNS.

contrast, stretching small-Wi polymers which have short relaxation times requires strong strain-rate events. These observations are consistent with a previous result by Terrapon *et al.* (2004) for a turbulent channel flow. It was shown that stretching events at low Wi are typically preceded by a burst of the strain rate; such bursts were not seen at high Wi.

If it is true that high-Wi polymers are stretched primarily by mild persistent straining, then they should not only stretch more in a Gaussian flow but also remain in an extended configuration for a longer duration of time. To detect this behaviour, we carry out a persistence time analysis and quantitatively compare how long polymers stay stretched in the turbulent and Gaussian random flows. Interestingly, the concept of persistence, which arose out of problems in non-equilibrium statistical physics (Majumdar 1999; Bray *et al.* 2013), has recently been used to study the turbulent transport of particles and filaments (Perlekar *et al.* 2011; Kadoch *et al.* 2011; Bhatnagar *et al.* 2016; Singh, Picardo & Ray 2022).

We begin by defining a polymer to be in a 'stretched' state if $R > \ell$, where the threshold $\ell = R_m/2$ is set well-within the power-law range. The non-stretched state is then defined as $R \leqslant \ell$. We have verified that varying the value of ℓ within the power-law range does not change our conclusions. With these states defined, we examine the Lagrangian history of each polymer and detect the time intervals t_{str} over which the polymer remains in a stretched state (see figure 3*b*). The distribution of this persistence time, $p(t_{str})$, is presented in figure 3(*c*) for various *Wi* and for both the turbulent and Gaussian flows. At large t_{str} the distribution displays an exponential tail, $p(t_{str}) \sim \exp(-t_{str}/T_{str})$, from which we extract the persistence time scale T_{str}.

Figure 3(*d*) presents T_{str} for both flows and for various values of *Wi*. Clearly, polymers with $Wi > Wi_{cr}$ typically remain stretched for a significantly longer time in the Gaussian flow as compared to the turbulent flow. This is true even for very large *Wi* for which the exponent of the power-law of $p(R)$ is nearly the same in both flows (see the results for $Wi \geqslant 2$ in figures 2*b* and 3*d*). So though the probability of large extensions is the same, the nature of stretching is different: Polymers experience many short-lived episodes of large extension in the turbulent flow, whereas such episodes are fewer but last longer in the Gaussian flow.

4. Temporal evolution of the distribution of polymer extensions

4.1. *Two regimes of evolution*

Thus far we have been studying the stationary p.d.f. of R, attained after the polymers have spent enough time in the flow for their statistics to equilibrate. We now examine how the p.d.f. of R evolves with time. Past work has shown that the p.d.f. relaxes exponentially to its stationary form, with a *Wi*-dependent time scale that exhibits a pronounced maximum at the coil–stretch transition (Celani *et al.* 2006; Watanabe & Gotoh 2010). But what is the shape of the p.d.f. as it evolves? And how, if at all, does this evolution depend on *Wi*?

To answer these questions, we use our Lagrangian simulations to construct the p.d.f. of R as a function of time, $p(R, t)$. We consider an initial state in which the polymers are in equilibrium with a static fluid. And so we first evolve the polymers with $\kappa = 0$ (in (2.1)) until the p.d.f. of R attains the equilibrium distribution (Bird *et al.* 1987). We then 'turn on' the turbulent flow.

The evolution of $p(R, t)$ is illustrated in figure 4. Interestingly, we find two qualitatively distinct regimes. At small or moderate *Wi* (figure 4*a*), the p.d.f. is seen to quickly attain a power-law form with an exponent $\beta(t)$ that increases in time until it reaches its stationary value $\beta_\infty = -1 - \alpha$. By fitting the distributions with a power law in the range $R_{eq} \ll R \ll R_m$, we find that $\beta(t)$ relaxes exponentially, *i.e.* $\beta_\infty - \beta \sim \exp(-t/T_\beta)$, as demonstrated in figure 4(*b*). The time-scale T_β is analyzed later in § 4.3.

The evolution at high *Wi* is quite different and is shown in figure 4(*c*)-(*d*). Here, the polymers stretch rapidly and quickly produce a local peak close to the maximum extension R_m. Thus, although a transient power law appears at very early times, it is quickly lost as the local peak at R_m begins to dominate the distribution (figure 4*c*). The long-time equilibration of the p.d.f. occurs by the peak near R_m first approaching its stationary value; then the stationary power law R^{β_∞} gradually emerges, starting near R_m and then extending its range down-scale towards R_{eq} (figure 4*d*).

These two regimes of equilibration are termed the *evolving power-law* regime and the *rapid-stretching* regime. The former occurs for $Wi \lesssim 3/4$, while the latter occurs for larger *Wi*. Note that the cross-over point, $Wi = 3/4$, is marked by a stationary p.d.f. with $\beta_\infty = 0$ that has neither a decaying tail at large R nor a local peak near R_m; the evolution near $Wi = 3/4$ is a blend of the two regimes.
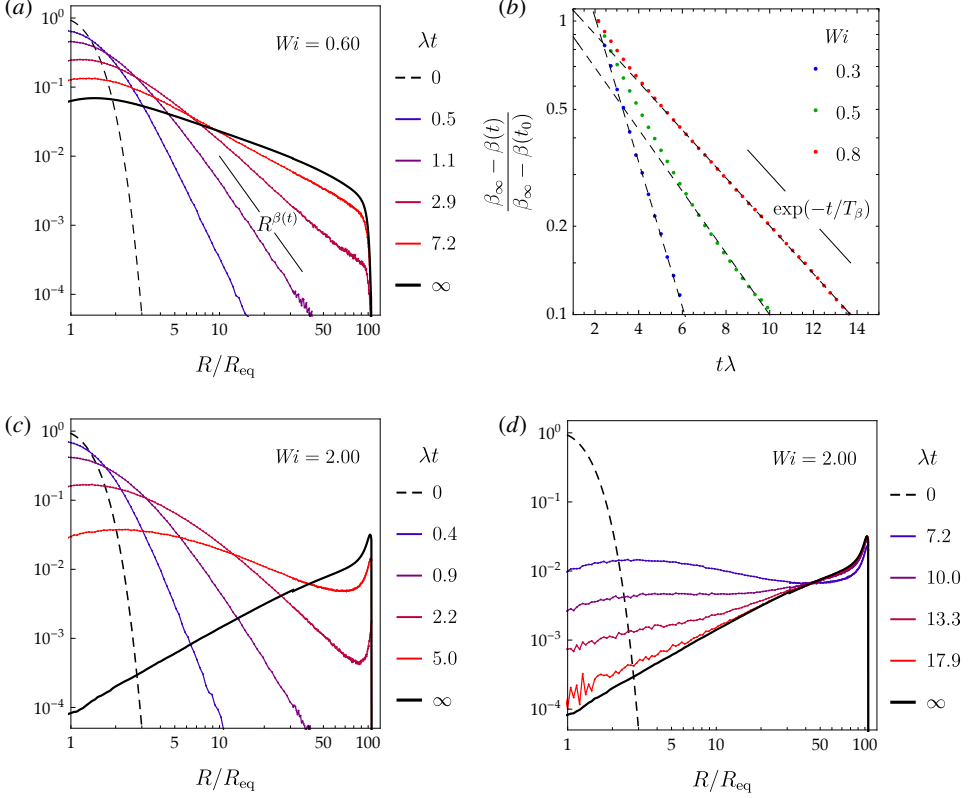
FIG. 4. Two regimes of evolution of the p.d.f. of the polymer extension. (*a*) Depiction of the *evolving power-law* regime, seen for small to moderate *Wi*, in which the tail of $p(R, t)$ evolves as $R^{\beta(t)}$. The thick black line with the time stamp $\lambda t = \infty$ represents the stationary p.d.f. of R. (*b*) The power-law exponent $\beta(t)$ is seen to approach its steady state value $\beta_\infty = -1 - \alpha$ exponentially. Here, t_0 is a reference time. (*c*)-(*d*) Depiction of the high-*Wi rapid stretching* regime, in which $p(R, t)$ does not evolve as a power law; rather the p.d.f. quickly forms a local maximum near to R_m (panel *c*) and then adjusts its shape directly to that of the stationary power law (panel *d*).

4.2. *The time-dependent power-law: insights from a stochastic model*

We now lend credence to the above characterization of the evolving power-law regime by using a stochastic model to show that, for $0 \leqslant Wi \lesssim 3/4$, an evolving power-law is a natural consequence of scale separation between $R_{\rm eq}$ and R_m. The associated analysis also reveals the *Wi* dependence of the relaxation time-scale T_β.

We consider the Batchelor–Kraichnan flow wherein the velocity gradient $\boldsymbol{\kappa}(t)$ is a statistically isotropic, time-decorrelated, 3×3 Gaussian tensor (Falkovich *et al.* 2001). In terms of the scaled variables $r = R/R_{\rm eq}$ and $\tilde{t} = t/2\tau$, the p.d.f. of the extension $p(r, \tilde{t})$ is governed by a Fokker–Planck equation (Martins Afonso & Vincenzi 2005; Plan *et al.* 2016):

$$\partial_{\tilde{t}} p = -\partial_r [D_1(r)p] + \partial_r^2 [D_2(r)p], \tag{4.1}$$

where $f(r) = 1/(1 - r^2/r_m^2)$, $r_m = R_m/R_{\rm eq}$, and

$$D_1(r) = [8Wi/3 - f(r)]r + 2/(3r), \quad D_2(r) = 2Wi\, r^2/3 + 1/3. \tag{4.2}$$

Note that while (4.1) is exact for the Batchelor–Kraichnan flow, an equation of the same form may be obtained for general turbulent flows by considering the Fokker–Planck equation associated with (2.1), assuming statistical isotropy, and modelling the stretching term *à la* Richardson, *i.e.*

as a diffusive process. The associated extension-dependent eddy diffusivity should scale as R^2 since the extension remains below the viscous scale.

We assume a wide separation between the scales of the equilibrium and maximum extensions, i.e. $R_m \gg R_{eq}$, or $r_m \gg 1$. Further, we focus on the long-time evolution of $p(r, \tilde{t})$ which is characterized by distinct behaviours for small, intermediate, and very large extensions: (i) In the range of extensions where thermal fluctuations dominate ($r < 1$), the p.d.f. of r assumes a quadratic profile (figure 2); (ii) For intermediate extensions $1 \ll r \ll r_m$, a power-law solution $r^{\beta(\tilde{t})}$ forms with an exponent $\beta(\tilde{t})$ that converges to its stationary value β_∞; (iii) For extreme extensions, $p(r, \tilde{t})$ decreases rapidly as r approaches r_m. We therefore introduce the ansatz:

$$p(r, \tilde{t}) \sim \begin{cases} c(\tilde{t})\, r^2 & (0 \leqslant r \leqslant 1), & (4.3a) \\ c(\tilde{t})\, r^{\beta(\tilde{t})} & (1 < r < \gamma r_m), & (4.3b) \\ g(r, \tilde{t}) & (\gamma r_m \leqslant r \leqslant r_m). & (4.3c) \end{cases}$$

Here, γ is a threshold value of r/r_m, less than unity, beyond which the nonlinear part of the FENE spring coefficient $f(r)$ becomes non-negligible and terminates the power-law behaviour. The function $g(r, \tilde{t})$ is such that, for $r = \gamma r_m$, we have $g(\gamma r_m, \tilde{t}) = c(\tilde{t})(\gamma r_m)^{\beta(\tilde{t})}$; while for $r > \gamma r_m$, $g(r, \tilde{t})$ decreases faster than $r^{\beta(\tilde{t})}$ as r approaches r_m. The latter assumption only applies if $Wi < 3/4$, for which $\beta_\infty < 0$. For larger Wi, our Lagrangian simulations show that the p.d.f. of r develops a pronounced time-dependent peak between γr_m and r_m (see figures 4c and 4d). Thus, the subsequent analysis applies only for $Wi < 3/4$, which in fact corresponds to the regime in which the Lagrangian simulations exhibit an evolving power law.

The coefficient $c(\tilde{t})$ is determined in terms of the exponent $\beta(\tilde{t})$ through the normalization condition

$$1 = \underbrace{\int_0^1 c(\tilde{t})r^2 \mathrm{d}r}_{I_1} + \underbrace{\int_1^{\gamma r_m} c(\tilde{t})r^{\beta(\tilde{t})} \mathrm{d}r}_{I_2} + \underbrace{\int_{\gamma r_m}^{r_m} g(r, \tilde{t}) \mathrm{d}r}_{I_3}. \qquad (4.4)$$

Clearly, $I_1 = c/3$, while $I_2 = c[(\gamma r_m)^{1+\beta} - 1]/[1 + \beta]$ for $\beta \neq 1$ and $I_2 = c \ln(\gamma r_m)$ for $\beta = -1$. For $r_m \gg 1$, I_3 is subdominant with respect to I_1 and I_2 and will be ignored. Thus, solving (4.4) for c yields

$$c = \frac{1 + \beta}{(\gamma r_m)^{1+\beta} + (\beta - 2)/3}, \quad \text{for } \beta \neq -1, \qquad (4.5a)$$

$$c = \frac{1}{1/3 + \ln(\gamma r_m)}, \qquad \text{for } \beta = -1. \qquad (4.5b)$$

To calculate $\beta(\tilde{t})$, we observe that, for $1 \ll r \ll r_m$, (4.1) can be simplified as follows:

$$\partial_t p = -\partial_r \left[\left(\frac{8}{3}Wi - 1 \right) r p \right] + \partial_r^2 \left(\frac{2}{3}Wi\, r^2 p \right). \qquad (4.6)$$

At steady-state we know that $p(r) \propto r^{\beta_\infty}$, which when substituted into (4.6) yields $\beta_\infty = 2 - 3/2Wi$, in accordance with the large deviations theory for a time-decorrelated flow (see (3.5) and recall that $\beta_\infty = -1 - \alpha$).

Now, substituting p from (4.3b) into (4.6) results in

$$\left(\frac{\mathrm{d}c}{\mathrm{d}\beta} + c \ln r \right) \frac{\mathrm{d}\beta}{\mathrm{d}\tilde{t}} = cF(\beta, Wi) \qquad (4.7)$$

with

$$F(\beta, Wi) = -\left(\frac{8}{3}Wi - 1 \right)(1 + \beta) + \frac{2}{3}Wi(1 + \beta)(2 + \beta). \qquad (4.8)$$

The left hand side of (4.7) contains $\mathrm{d}c/\mathrm{d}\beta$ which is evaluated using (4.5):

$$\frac{\mathrm{d}c}{\mathrm{d}\beta} = c\left[\frac{1}{1+\beta} - \frac{(\gamma r_m)^{1+\beta}\ln{(\gamma r_m)} + 1/3}{(\gamma r_m)^{1+\beta} + (\beta-2)/3}\right], \quad \text{for } \beta \neq -1, \tag{4.9a}$$

$$\frac{\mathrm{d}c}{\mathrm{d}\beta} = 0, \qquad \text{for } \beta = -1. \tag{4.9b}$$

On taking the limit $r_m \gg 1$, the right-hand-side of (4.9a) simplifies to $-3c/(\beta^2 - \beta - 2)$ for $\beta < -1$ and to $-c\ln{(\gamma r_m)}$ for $\beta > -1$. By substituting these expressions for $\mathrm{d}c/\mathrm{d}\beta$ in (4.7) and considering that $r_m \gg r \gg 1$, we obtain the following leading-order equation for β:

$$\ln(r)\frac{\mathrm{d}\beta}{\mathrm{d}\tilde{t}} = F(\beta, Wi), \qquad \text{for } \beta \leqslant -1, \tag{4.10a}$$

$$\ln(\gamma r_m)\frac{\mathrm{d}\beta}{\mathrm{d}\tilde{t}} = -F(\beta, Wi), \quad \text{for } \beta > -1. \tag{4.10b}$$

Because $\ln{(x)}$ is a weak function of x for $x \gg 1$, we approximate $\ln r$ in (4.10a), as well as $\ln(\gamma r_m)$ in (4.10b), as $\ln r_m$ to obtain

$$\frac{\mathrm{d}\beta}{\mathrm{d}\tilde{t}} \approx a\,\frac{F(\beta, Wi)}{\ln r_m}, \tag{4.11}$$

with $a = 1$ for $\beta \leqslant -1$ and $a = -1$ for $\beta > -1$.

Being independent of r, (4.11) shows that $p(R, t)$ may be approximated (up to logarithmic corrections) by a time-dependent power-law in the range $R_{\mathrm{eq}} \ll R \ll R_m$.

Next, to reveal the long-time relaxation of β to β_∞, we substitute $\beta = \beta_\infty + \beta'$ in (4.11) and linearize for small β'. Noting that $F(\beta_\infty, Wi) = 0$ and that $\beta_\infty < -1$ for $Wi < Wi_{\mathrm{cr}}$, we obtain

$$\frac{\mathrm{d}\beta'}{\mathrm{d}\tilde{t}} = -\frac{2\,(Wi_{\mathrm{cr}} - Wi)}{\ln r_m}\beta', \quad \text{for } Wi < Wi_{\mathrm{cr}}, \tag{4.12a}$$

$$\frac{\mathrm{d}\beta'}{\mathrm{d}\tilde{t}} = -\frac{2\,(Wi - Wi_{\mathrm{cr}})}{\ln r_m}\beta', \quad \text{for } Wi_{\mathrm{cr}} < Wi < 3/4. \tag{4.12b}$$

In terms of dimensional time t, this implies an exponential relaxation of the power-law exponent,

$$\beta_\infty - \beta(t) \sim \exp(-t/T_\beta), \tag{4.13}$$

with a time scale

$$T_\beta \sim \frac{\tau}{|Wi - Wi_{\mathrm{cr}}|} \tag{4.14}$$

that diverges as Wi approaches Wi_{cr}.

Note that (4.11) actually has two fixed points: β_∞ and -1. The latter, though, can be shown to be dynamically unstable, leaving β_∞ as the only stable fixed point.

The prediction (4.13) of an exponentially relaxing power-law exponent is certainly in agreement with the results of our Lagrangian simulations (see figure 4b). The Wi-dependence of the relaxation time-scale will be examined in light of (4.14) in the next section. But first, it is instructive to compare (4.13)-(4.14) against numerical simulations of the Fokker-Planck equation (4.1). Beginning from a distribution of coiled dumbbells, we solve (4.1) using second-order central differences and the LSODA algorithm (Petzold 1983) with adaptive time-stepping (Wolfram Research 2019). We take $R_m = 10^3 R_{\mathrm{eq}}$, thereby realizing a much larger scale separation than is practical in our Lagrangian simulations. The results are presented in figure 5.

The stochastic model exhibits the same two regimes of evolution as the Lagrangian simulations: the evolving power-law regimes for $Wi < 3/4$ (cf. figures 4a and 5a) and the rapid-stretching regime for larger Wi (cf. figures 4c-4d and 5b). Within the evolving power-law regime, we extract the exponent $\beta(t)$ and find that it does in fact evolve exponentially, in accordance with (4.13). The
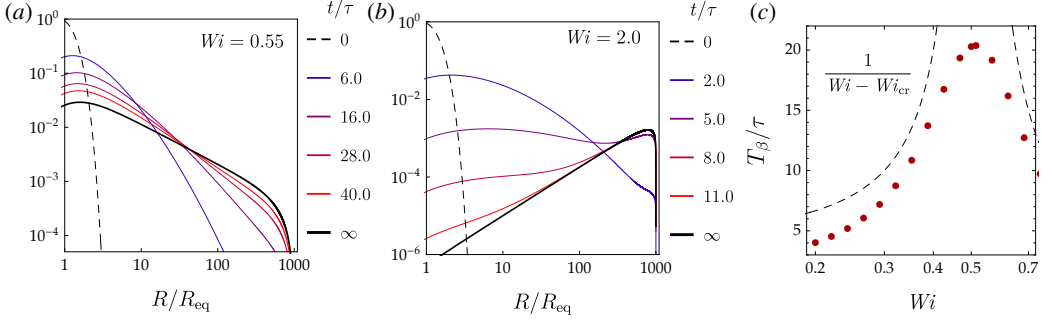
FIG. 5. Evolution of the p.d.f. of the extension as predicted by numerical simulations of the Fokker–Planck equation for the Batchelor–Kraichnan flow (with $R_m = 10^3 R_{eq}$). The evolving power-law regime is shown in panel (*a*), while the rapid-stretching regime is shown in panel (*b*). The time-scale of relaxation T_β of the evolving power-law exponent is shown in panel (*c*) as a function of *Wi*. The dashed line shows the variation predicted by the asymptotic analysis [cf. (4.13)].

time-scale T_β, obtained from a least-squares fit, is presented as a function of *Wi* in figure 5(*c*). The predicted divergence of T_β at Wi_{cr} (see (4.14)), manifests in the simulations (which have a finite scale separation) as a prominent maximum of T_β at Wi_{cr}. Such a slowing down of the stretching dynamics at the coil–stretch transition was demonstrated by Martins Afonso & Vincenzi (2005) and Celani *et al.* (2006), but in regard to the equilibration of the entire p.d.f. of *R*. The behaviour of T_β vs *Wi* gives an alternative characterization of the same phenomenon.

4.3. *Temporal correlation and non-Gaussian statistics slow the equilibration of $p(R,t)$*

We now quantitatively compare the time scales of equilibration of $p(R,t)$ in the turbulent and Gaussian flows (Lagrangian simulations) as well as in the Batchelor–Kraichnan decorrelated flow (numerical solution of the stochastic model).

One time scale of interest is that associated with the evolving power-law tail, T_β. However, this time scale is only relevant for $Wi < 3/4$. So, to characterize the equilibration time for all *Wi*, we use the time scale associated with the entire p.d.f. of *R*. Martins Afonso & Vincenzi (2005) and Celani *et al.* (2006) showed, for random flows, that $p(R,t)$ approaches its asymptotic stationary form exponentially, with a time-scale T_P that displays a maximum near Wi_{cr}. Watanabe & Gotoh (2010) confirmed this prediction in a DNS of isotropic turbulence. We obtain T_P from our simulations by fitting the evolution of the first moment of $p(R,t)$ (approximately the same value is obtained by fitting the higher moments).

Figure 6 compares the equilibration time scales T_β and T_P in panels (*a*) and (*b*), respectively, for the turbulent flow (filled markers) and the Gaussian flow (open markers). The results for the time-decorrelated Batchelor–Kraichnan flow are also presented (line). We see that the qualitative variation of these time scales with *Wi* is the same in all flows and exhibits a maximum near Wi_{cr}. In the case of T_P, a Wi^{-1} asymptotic behaviour is visible (see the inset of figure 6*b*), in agreement with Martins Afonso & Vincenzi (2005) and Celani *et al.* (2006).

On comparing the results for the Gaussian and decorrelated flows, we see that the time correlation of the flow slows down the equilibration of the p.d.f. of *R*: both T_β and T_P are higher for the Gaussian flow (figures 6*a* and 6*b*). The equilibration is even slower for the turbulent flow (DNS) with its non-Gaussian velocity gradient statistics.

Qualitatively, chaotic random flows are seen to provide a good approximation for studying polymer stretching in homogeneous isotropic turbulence. Our results also show that the accuracy of the predictions, especially for finite-time statistics, are improved by incorporating temporal correlation in the random flow.
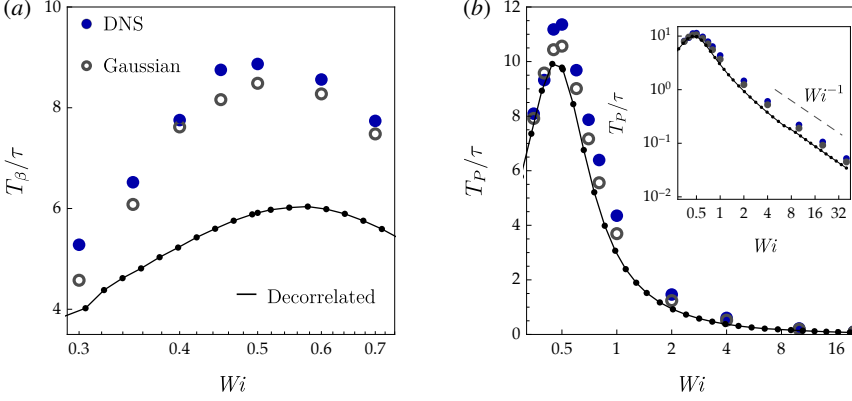
FIG. 6. Effect of non-Gaussian velocity-gradient statistics on the time scale of evolution of the p.d.f. of the extension to its stationary form. (*a*) Comparison of the relaxation time scale T_β of the power-law exponent of the tail of the p.d.f. of R obtained from DNS (cf. figure 4*b*) with that from the synthetic Gaussian flow as well as the Batchelor–Kraichnan flow (simulations of (4.1)). (*b*) Comparison of the exponential relaxation time scale T_P of the entire p.d.f. of R, for the three different cases: DNS, Gaussian flow, and Batchelor–Kraichnan flow. The inset is a log-log plot of the same data which shows the Wi^{-1} asymptotic behaviour.

5. Chains stretch like equivalent dumbbells

Thus far we have focused on the simplest model for a polymer of finite extension, the FENE dumbbell (§ 2.1). We now show that the key results presented above also hold for a polymer chain, which incorporates higher-order deformation modes.

The three-dimensional motion of a freely-jointed (Rouse) chain, composed of $\mathcal{N}$ beads, is described in terms of the position of its center of mass, X_c, and the separation vectors between the beads, Q_i ($i = 1, \ldots, \mathcal{N} - 1$) (Bird *et al.* 1987; Öttinger 1996):

$$\dot{X}_c = u(X_c(t), t) + \frac{1}{\mathcal{N}} \sqrt{\frac{Q_{\text{eq}}^2}{6\tau_*}} \sum_{i=1}^{\mathcal{N}} \xi_i(t), \tag{5.1a}$$

$$\dot{Q}_i = \kappa(t) \cdot Q_i(t) - \frac{1}{4\tau_*} [2f_i Q_i(t) - f_{i+1} Q_{i+1}(t) - f_{i-1} Q_{i-1}(t)] \tag{5.1b}$$

$$+ \sqrt{\frac{Q_{\text{eq}}^2}{6\tau_*}} [\xi_{i+1}(t) - \xi_i(t)], \qquad i = 1, \ldots, \mathcal{N} - 1,$$

where each link is associated with an elastic time scale τ_* and has an equilibrium r.m.s. extension $Q_{\text{eq}} = \sqrt{3k_B T/H}$. The FENE interactions between neighbouring beads is characterized by the coefficients

$$f_i = \frac{1}{1 - |Q_i|^2/Q_m^2}, \tag{5.2}$$

which ensure that the extension of each spring does not exceed its maximum length Q_m. The Brownian forces that act on the beads are represented by independent, vectorial, white noises $\xi_i(t)$. Note that one must set $Q_0 = Q_{\mathcal{N}} = 0$ in the equations for Q_1 and $Q_{\mathcal{N}-1}$.

The end-to-end separation or extension vector of the polymer chain is defined as $R = \sum_{i=1}^{\mathcal{N}-1} Q_i$. In a still fluid, the equilibrium r.m.s. value of $|R|$ is $Q_{\text{eq}} \sqrt{\mathcal{N} - 1}$ (Bird *et al.* 1987).

In order to compare the extensional dynamics of a chain and a dumbbell, Jin & Collins (2007)
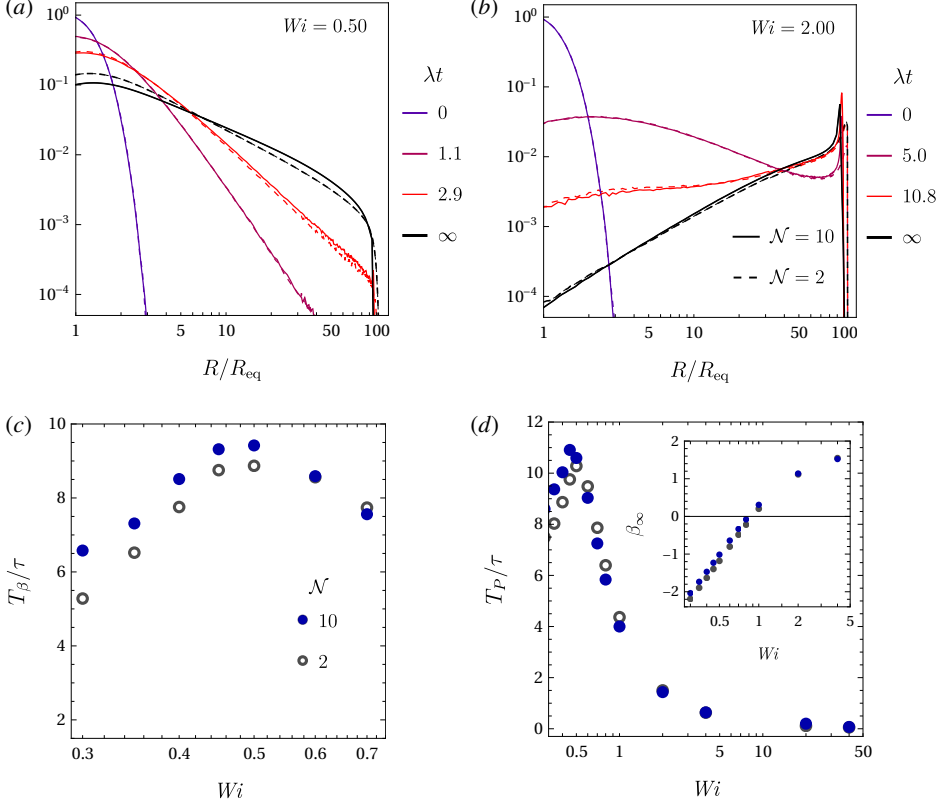
FIG. 7. Effect of the polymer model—bead-spring dumbbell or chain—on the evolution of the p.d.f. of the extension. (*a*) Comparison of the evolving p.d.f. of *R*, in the evolving power-law regime, of a $\mathcal{N} = 10$ chain (solid line) with that of an equivalent dumbbell (dashed line). The parameters of the dumbbell are given by (5.3). (*b*) Comparison of the evolution of the p.d.f. of *R* in the rapid stretching regime. (*c*) Comparison of the relaxation time T_β of the power-law exponent of the evolving p.d.f. for the chain and dumbbell and for various *Wi* in the evolving-power-law regime. (*d*) Comparison of the exponential relaxation time-scale T_P of the entire p.d.f. of *R* for the chain and the dumbbell. The inset compares the power-law exponents of the stationary p.d.f.s.

proposed the following mapping between the parameters of the two models:

$$R_{\text{eq}} = Q_{\text{eq}}\sqrt{\mathcal{N} - 1}, \quad R_m = Q_m\sqrt{\mathcal{N} - 1}, \quad \tau = \frac{(\mathcal{N} + 1)\mathcal{N}}{6}\tau_*. \quad (5.3)$$

This map is obtained by starting with the relation between R_{eq} and Q_{eq}, which follows from the random-walk theory for a polymer in a still fluid (de Gennes 1979), and then using it in an expression for the elongational viscosity of highly-stretched polymers given by Wiest & Tanner (1989). By requiring the value of the viscosity thus obtained to be independent of $\mathcal{N}$, one obtains the relation between the time-scale of the springs of an $\mathcal{N}$-bead chain, τ_*, and that of an equivalent dumbbell, τ (Jin & Collins 2007). This mapping was shown to work very well for the stationary p.d.f. of *R* by Watanabe & Gotoh (2010) (see the inset of figure 7*d* for a comparison of the power-law exponent corresponding to the stationary p.d.f.). Here, we check to see if it works equally well for the temporal evolution of the distribution.

Figure 7 compares the evolution and equilibration of the p.d.f. of *R* for a dumbbell and a $\mathcal{N} = 10$ chain. Panels (*a*) and (*b*) depict the evolution of $p(R, t)$ for a small and high *Wi*, respectively. The results agree quite well in both cases. Figure 7(*c*) compares the equilibration time-scale of

the evolving power-law, T_β, while figure 7(d) compares the equilibration time-scale of the entire p.d.f., T_P. While the results of the dumbbell and chain are similar for all Wi, they are in excellent agreement at high Wi. This is unsurprising, given that the mapping (5.3) was derived by equating the elongation viscosity of highly stretched chains and dumbbells (Jin & Collins 2007).

6. Concluding remarks

Polymers in a chaotic flow field stretch and coil repeatedly, sampling a broad distribution of extensions. The basic features of the stationary distribution—a power-law tail and the coil–stretch transition—are well documented and understood in terms of the large deviations theory. In this work, we have examined the stretching dynamics in more detail to understand how the stationary distribution of extensions is attained and how polymers respond to the non-Gaussian time-correlated velocity-gradient statistics of turbulence.

We have seen that extreme strain rates are important only for stretching stiff low-Wi polymers, whereas it is mild but persistent straining that extends more elastic high-Wi polymers. This insight has relevance for the extension of polymers in the presence of two-way coupling with the flow. The feedback forces exerted by polymers onto the flow not only reduce the mean value of the strain rate but also suppress its extreme-valued fluctuations (ur Rehman et $al.$ 2022; Perlekar et $al.$ 2010). Clearly, the reduction in the mean strain rate will cause two-way coupled polymers to stretch less, on average, than one-way coupled passive polymers. In fact, at large values of Wi, this effect can be strong enough to cause the mean extension to decrease with increasing Wi (Rosti et $al.$ 2021). But what if one compensates for the reduced mean value by suitable rescaling? Would we see a separate effect of the loss of extreme events, arising from just the change in the shape of the distribution of strain-rates? This question was addressed in recent Eulerian–Lagrangian simulations by ur Rehman et $al.$ (2022). They defined an effective Wi for two-way coupled polymers, using the reduced value of the Kolmogorov time scale of the modified flow, and then compared the stretching statistics of two-way and one-way coupled polymers. They found that the mean and standard deviation of the p.d.f. of extension are almost the same for one-way and two-way coupled polymers with the same effective Wi. This was despite the fact that the feedback forces were strong enough to substantially modify the net dissipation rate, as well as the statistics of vorticity and strain rate. This result is understandable, indeed is to be expected, in light of our results. At small Wi where extreme strain rates are important, the feedback force and thus the modification of the flow will be weak; at large Wi, the extreme strain rates are no longer important for stretching and their loss does not impact the extent of stretching. It should be noted that the simulations of ur Rehman et $al.$ (2022) were carried out at a low volume fraction; the impact of feedback forces on polymer stretching may differ at larger volume fractions.

Examining the time evolution of the p.d.f. of extensions, we have identified two regimes: the low-Wi evolving power-law regime and the high-Wi rapid stretching regime. In both regimes, the p.d.f. equilibrates exponentially with a time-scale that peaks near the coil–stretch transition. While performing experiments or simulations at low to moderate Wi, one should bear in mind that the non-stationary p.d.f. has the form of an evolving power law, so that the mere appearance of a power-law subrange is not construed as evidence for having attained stationarity.

The turbulent carrier flow used in our simulations has a Taylor-Reynolds number of $Re_\lambda \approx 111$; though modest, this value is sufficient for the strain rate to exhibit strongly non-Gaussian statistics (figure 3a). The comparison with a Gaussian random flow has shown that the higher frequency of extreme strain rates, encountered in turbulence, has no qualitative effect on polymer stretching. So, a further intensification of the extreme strain-rates by increasing Re_λ is unlikely to change the nature of stretching, although, the quantitative differences between the p.d.f. of extensions in the turbulent and Gaussian flows may be amplified.

While most of this work has considered the FENE dumbbell, we have shown that our results

are valid for a bead-spring chain as well. However, we have for simplicity neglected inter-bead hydrodynamics interactions (HI) and excluded volume (EV) forces. These forces do not play a role once polymers are stretched, but they do affect the time it takes for polymers to unravel (Schroeder *et al.* 2004; Sim *et al.* 2007; Vincenzi *et al.* 2021). Understanding their effect on individual polymer stretching and ultimately on the turbulent dynamics of polymer solutions is an important area for future work.

One of the challenges in developing accurate models for polymers that undergo rapid stretching in turbulence is the large computational cost involved in simulating complex polymer chains in a turbulent flow. This difficulty would be greatly reduced if the DNS for the flow is replaced by a random flow field. The results of our study show that this would indeed be a useful strategy, because the stretching dynamics have been shown to be only mildly sensitive to the detailed statistics of the flow. For example, one could use a time-correlated Gaussian velocity gradient for testing the consequence of including forces like EV and HI, and for developing coarse-grained effective dumbbell models. The latter could then be used for Lagrangian simulations in a DNS of turbulent polymer solutions.

Declaration of interests. The authors report no conflict of interest.

Author ORCID J. R. Picardo, https://orcid.org/0000-0002-9227-5516; E. L. C. VI M. Plan, https://orcid.org/0000-0003-2268-424X; D. Vincenzi, https://orcid.org/0000-0003-3332-3802

References

Anand, P., Ray, S. S. & Subramanian, G. 2020 Orientation dynamics of sedimenting anisotropic particles in turbulence. *Phys. Rev. Lett.* **125**, 034501.

Bagheri, F., Mitra, D., Perlekar, P. & Brandt, L. 2012 Statistics of polymer extensions in turbulent channel flow. *Phys. Rev. E* **86**, 056314.

Balkovsky, E., Fouxon, A. & Lebedev, V. 2000 Turbulent dynamics of polymer solutions. *Phys. Rev. Lett.* **84**, 4765–4768.

Balkovsky, E., Fouxon, A. & Lebedev, V. 2001 Turbulence of polymer solutions. *Phys. Rev. E* **64**, 056301.

Bec, J., Biferale, L., Boffetta, G., Cencini, M., Musacchio, S. & Toschi, F. 2006 Lyapunov exponents of heavy particles in turbulence. *Phys. Fluids* **18**, 091702.

Benzi, R. & Ching, E. S. C. 2018 Polymers in fluid flows. *Annu. Rev. Condens. Matter Phys.* **9**, 163–181.

Bhatnagar, A., Gupta, A., Mitra, D., Pandit, R. & Perlekar, P. 2016 How long do particles spend in vortical regions in turbulent flows? *Phys. Rev. E* **94**, 053119.

Biferale, L., Meneveau, C. & Verzicco, R. 2014 Deformation statistics of sub-Kolmogorov-scale ellipsoidal neutrally buoyant drops in isotropic turbulence. *J. Fluid Mech.* **754**, 184–207.

Bird, R. B., Curtiss, C. F., Armstrong, R. C. & Hassager, O. 1987 *Dynamics of Polymeric Liquids*, , vol. 2. Wiley.

Boffetta, G., Celani, A. & Musacchio, S. 2003 Two-dimensional turbulence of dilute polymer solutions. *Phys. Rev. Lett.* **91**, 034501.

Bray, Alan J., Majumdar, Satya N. & Schehr, Grégory 2013 Persistence and first-passage properties in nonequilibrium systems. *Advances in Physics* **62** (3), 225–361.

Brunk, B. K., Koch, D. L. & Lion, L. W. 1997 Hydrodynamic pair diffusion in isotropic random velocity fields with application to turbulent coagulation. *Phys. Fluids* **9**, 2670–2691.

Cecconi, F., Cencini, M. & Vulpiani, A. 2010 *Chaos: from Simple Models to Complex Systems*. Singapore: World Scientific.

Celani, A., Puliafito, A. & Vincenzi, D. 2006 Dynamical slowdown of polymers in laminar and random flows. *Phys. Rev. Lett.* **97**, 118301.

Chertkov, M. 2000 Polymer stretching by turbulence. *Phys. Rev. Lett.* **84**, 4761–4764.

Chevillard, L. & Meneveau, C. 2013 Orientation dynamics of small, triaxial–ellipsoidal particles in isotropic turbulence. *J. Fluid Mech.* **737**, 571–596.

Childress, S. & Gilbert, A. D. 1995 *Stretch, Twist, Fold: The Fast Dynamo*. Berlin: Springer.

Dieci, L., Russell, R. D. & Vleck, E. S. Van 1997 On the computation of Lyapunov exponents for continuous dynamical systems. *SIAM J. Numer. Anal.* **34**, 402–423.

Eckhardt, B., Kronjäger, J. & Schumacher, J. 2002 Stretching of polymers in a turbulent environment. *Comput. Phys. Commun.* **147**, 538–543.

Falkovich, G., Gawędki, K. & Vergassola, M. 2001 Particles and fields in fluid turbulence. *Rev. Mod. Phys.* **73**, 913–975.

Frisch, U. 1995 *Turbulence: The Legacy of A. N. Kolmogorov*. Cambridge, England: Cambridge University Press.

de Gennes, P.-G. 1979 *Scaling Concepts in Polymer Physics*. Ithaca, NY: Cornell University Press.

Gerashchenko, S, Chevallard, C. & Steinberg, V. 2005 Single-polymer dynamics: Coil-stretch transition in a random flow. *Europhys. Lett.* **71**, 221–227.

Gerashchenko, S & Steinberg, V. 2008 Critical slowing down in polymer dynamics near the coil-stretch transition in elongation flow. *Phys. Rev. E* **78**, 040801(R).

Graham, M. D. 2014 Drag reduction and the dynamics of turbulence in simple and complex fluids. *Phys. Fluids* **26**, 101301.

Graham, M. D. 2018 *Microhydrodynamics, Brownian Motion, and Complex Fluids*. Cambridge, UK: Cambridge University Press.

Groisman, A. & Steinberg, V. 2001 Stretching of polymers in a random three-dimensional flow. *Phys. Rev. Lett.* **86**, 934–937.

Gupta, A., Perlekar, P. & Pandit, R. 2015 Two-dimensional homogeneous isotropic fluid turbulence with polymer additives. *Phys. Rev. E* **91**, 033013.

Gupta, V. K., Sureshkumar, R. & Khomami, B. 2004 Polymer chain dynamics in Newtonian and viscoelastic turbulent channel flows. *Phys. Fluids* **16**, 1546.

Gustavsson, K., Einarsson, J. & Mehlig, B. 2014 Tumbling of small axisymmetric particles in random and turbulent flows. *Phys. Rev. Lett.* **112**, 014501.

Ilg, P., Angelis, E. De, Karlin, I. V., Casciola, C. M. & Succi, S. 2002 Polymer dynamics in wall turbulent flow. *Europhys. Lett.* **58**, 616.

James, M. & Ray, S. S. 2017 Enhanced droplet collision rates and impact velocities in turbulent flows: The effect of poly-dispersity and transient phases. *Sci. Reports* **7**, 12231.

Jin, S. & Collins, L. R. 2007 Dynamics of dissolved polymer chains in isotropic turbulence. *New J. Phys.* **9**, 360.

Kadoch, B., del Castillo-Negrete, D., Bos, W. J. T. & Schneider, K. 2011 Lagrangian statistics and flow topology in forced two-dimensional turbulence. *Phys. Rev. E* **83**, 036314.

Liu, Y. & Steinberg, V. 2010 Stretching of polymer in a random flow: Effect of a shear rate. *Europhys. Lett.* **90**, 44005.

Liu, Y. & Steinberg, V. 2014 Single polymer dynamics in a random flow. *Macromol. Symp.* **337**, 34–43.

Lumley, J. L. 1973 Drag reduction in turbulent flow by polymer additives. *J. Polymer Sci. Macromol. Rev.* **7**, 263–290.

Majumdar, S. N. 1999 Persistence in nonequilibrium systems. *Current Science* **77** (3), 370–375.

Martins Afonso, M. & Vincenzi, D. 2005 Nonlinear elastic polymers in random flow. *J. Fluid Mech.* **540**, 99–108.

Massah, H., Kontomaris, K., Schowalter, W. R. & Hanratty, T. J. 1993 The configurations of a FENE bead-spring chain in transient rheological flows and in a turbulent flow. *Phys. Fluids A* **5**, 881.

Mosler, A. B. & Shaqfeh, E. S. G. 1997 The conformation change of model polymers in stochastic flow fields: Flow through fixed beds. *Phys. Fluids* **9**, 1222.

Nguyen, T. Q. & Kausch, H.-H., ed. 1999 *Flexible Polymer Chain Dynamics in Elongational Flow*. Berlin Heidelberg: Springer.

Öttinger, H. C. 1996 *Stochastic Processes in Polymeric Fluids*. Berlin: Springer.

Perkins, T., Smith, D. E. & Chu, S. 1997 Single polymer dynamics in an elongational flow. *Science* **276**, 2016–2021.

Perlekar, P., Mitra, D. & Pandit, R. 2010 Direct numerical simulations of statistically steady, homogeneous, isotropic fluid turbulence with polymer additives. *Phys. Rev. E* **82**, 066313.

Perlekar, P., Ray, S. S., Mitra, D. & Pandit, R. 2011 Persistence problem in two-dimensional fluid turbulence. *Phys. Rev. Lett.* **106**, 054501.

Peters, T. & Schumacher, J. 2007 Two-way coupling of finitely extensible nonlinear elastic dumbbells with a turbulent shear flow. *Phys. Fluids* **19**, 065109.

Petzold, L. 1983 Automatic selection of methods for solving stiff and nonstiff systems of ordinary differential equations. *SIAM Journal on Scientific and Statistical Computing* **4** (1), 136–148.

Plan, E. L. C. VI M., Ali, A. & Vincenzi, D. 2016 Bead-rod-spring models in random flows. *Phys. Rev. E* **94**, 020501(R).

Puliafito, A. & Turitsyn, K. 2005 Numerical study of polymer tumbling in linear shear flows. *Physica D* **211**, 9–22.

Pumir, A. & Wilkinson, M. 2011 Orientation statistics of small particles in turbulence. *New J. Phys.* **13**, 093030.

ur Rehman, S., Lee, J. & Lee, C. 2022 Effect of Weissenberg number on polymer-laden turbulence. *Phys. Rev. Fluids* **7**, 064303.

Rosti, M. E., Perlekar, P. & Mitra, D. 2021 Large is different: non-monotonic behaviour of elastic range scaling in polymeric turbulence at large Reynolds and Deborah numbers. `arXiv:2111.11224`.

Schroeder, C. M. 2018 Single polymer dynamics for molecular rheology. *J. Rheol.* **62**, 371–403.

Schroeder, C. M., Babcock, H. P., Shaqfeh, E. S. G. & Chu, S. 2003 Observation of polymer conformation hysteresis in extensional flow. *Science* **301**, 1515–1519.

Schroeder, C. M., Shaqfeh, E. S. G. & Chu, S. 2004 Effect of hydrodynamic interactions on dna dynamics in extensional flow: Simulation and single molecule experiment. *Macromolecules* **37**, 9242–9256.

Serafini, F., Battista, F., Gualtieri, P. & Casciola, C. M. 2022 Drag reduction in turbulent wall-bounded flows of realistic polymer solutions. *Phys. Rev. Lett.* **129**, 104502.

Shaqfeh, E. S. G. & Koch, D. L. 1992 Polymer stretch in dilute fixed beds of fibres or spheres. *J. Fluid Mech.* **244**, 17–54.

Sim, H. G., Khomami, B. & Sureshkumar, R. 2007 Flow–induced chain scission in dilute polymer solutions: Algorithm development and results for scission dynamics in elongational flow. *J. Rheol.* **51** (6), 1223–1251.

Singh, R. K., Picardo, J. R. & Ray, S. S. 2022 Sedimenting elastic filaments in turbulent flows. *Phys. Rev. Fluids* **7**, 084502.

Soares, E. J. 2020 Review of mechanical degradation and de-aggregation of drag reducing polymers in turbulent flows. *J. Non-Newtonian Fluid Mech.* **276**, 104225.

Steinberg, V. 2021 Elastic turbulence: An experimental view on inertialess random flow. *Annu. Rev. Fluid Mech.* **53**, 27–58.

Stone, P. A. & Graham, M. D. 2003 Polymer dynamics in a model of the turbulent buffer layer. *Phys. Fluids* **15**, 1247–1256.

Terrapon, V. E., Dubief, Y., Moin, P., Shaqfeh, E. S. G. & Lele, S. K. 2004 Simulated polymer stretch in a turbulent flow using Brownian dynamics. *J. Fluid Mech.* **504**, 61.

Vanneste, J. 2010 Estimating generalized Lyapunov exponents for products of random matrices. *Phys. Rev. E* **81**, 036701.

Vincenzi, D., Watanabe, T., Ray, S. S. & Picardo, J. 2021 Polymer scission in turbulent flows. *J. Fluid Mech.* **912**, A18.

Watanabe, T. & Gotoh, T. 2010 Coil-stretch transition in an ensemble of polymers in isotropic turbulence. *Phys. Rev. E* **81**, 066301.

Watanabe, T. & Gotoh, T. 2013 Hybrid Eulerian–Lagrangian simulations for polymer–turbulence interactions. *J. Fluid Mech.* **717**, 535–575.

Wiest, J. M. & Tanner, R. I. 1989 Rheology of bead-nonlinear spring chain macromolecules. *J. Rheol.* **33** (2), 281–316.

Wolfram Research 2019 NDSolve. https://reference.wolfram.com/language/ref/NDSolve.html.

Xi, L. 2019 Turbulent drag reduction by polymer additives: Fundamentals and recent advances. *Phys. Fluids* **31**, 121302.

Yeung, P. K. 2001 Lagrangian characteristics of turbulence and scalar transport in direct numerical simulations. *J. Fluid Mech.* **427**, 241–274.

Young, W. R. 1999 Stirring and mixing. In *1999 Summer Program in Geophysical Fluid Dynamics* (ed. J.-L. Thiffeault & C. Pasquero). Woods Hole Oceanographic Institution, Woods Hole, MA.

Young, W. R. 2009 The passive scalar problem. Institut Henri Poincaré, Paris, https://mhd.ens.fr/IHP09/Young/.

Zel'dovich, Ya. B., Ruzmaikin, A. A., Molchanov, S. A. & Sokoloff, D. D. 1984 Kinematic dynamo problem in a linear velocity field. *J. Fluid Mech.* **144**, 1–11.

Zhou, Q. & Akhavan, R. 2003 A comparison of FENE and FENE-P dumbbell and chain models in turbulent flow. *J. Non-Newtonian Fluid Mech.* **109**, 115.